

# Local Structural Studies of Magnetic Field Induced Melting of the Charge Ordered State of $\text{La}_{0.5}\text{Ca}_{0.5}\text{MnO}_3$

T. A. Tyson (NJIT)

## Collaborators

M. Deleon (NJIT)  
M. Croft (Rutgers U.)  
V. G. Harris (North Eastern)  
C.-C. Kao (NSLS, BNL)  
S.-W. Cheong (Rutgers U.)  
J. Kirkland (NRL)

# Outline

- Complex Properties of CMR Oxides
- Properties Half-Doped Region  $\text{Re}_{0.5}\text{A}_{0.5}\text{MnO}_3$  exemplified by  $\text{La}_{0.5}\text{Ca}_{0.5}\text{MnO}_3$
- Local Structural Changes during CO melting in  $\text{La}_{0.5}\text{Ca}_{0.5}\text{MnO}_3$
- Summary

## Complex Properties of CMR Oxides (Cubic System)

### Applications Perspective

The enhancement in information density is being effected by the following: the development of new magnetic recording materials; the reduction in the distance between the read-write head and the recording disk; the reduction in the magnetic bit -size; increases in the track density; and **increases in the sensitivity of the read-heads**. A new generation of devices which integrate both the spin and charge of electrons is making an impact in this field

The manganite system is being carefully studied due to the large magnetoresistance found in this system – However, the fields required are in the 100 Oe range while sensors require responses in the 100 Oe range

### Fundamental Physics Perspective

The manganites are a system which exhibits intimate spin, lattice and charge coupling which produce complicated phase diagrams. This system is a test bed for understanding strongly electron correlated systems (single electron in sea of ions is not valid).

## Properties – I(a)

- N. Mathur and P. Littlewood, Physics Today, January 2003; . M. B. Salamon and M. Jaime, Rev. Mod. Phys. **73**, 583 (2001); Y. Tokura and Y. Tomioka, JMMM **200**, 1 (1999); J. M. D. Coey, M. Viret and S. von Molnar, Adv. in Phys. **48**, 167 (1999). *Discovered in late 1940's (Jonker and van Santen) but interest was revived with observation of large magnetoresistance by Jin et al.*
- As a function of doping, using divalent cations A= Ca, Sr, Ba ... in place of the trivalent cation La, the average valence of Mn in  $\text{La}_{1-x}\text{A}_x\text{MnO}_3$  is predicted to vary from  $\text{Mn}^{3+}$  ( $x=0$ ) to  $\text{Mn}^{4+}$  ( $x=1$ ) corresponding to a change in the d valence from  $d^4$  to  $d^3$

## Properties – I(b)

- The degenerate  $\text{Mn}^{3+}$  state is known to be unstable with respect to Jahn-Teller (JT) distortions (M. D. Struge, Jahn Teller Effect in the  ${}^4\text{T}_{2g}$  Excited state of  $\text{V}^{2+}$  in  $\text{MgO}^+$ , Phys. Rev. **140**, A880 (1965) and references therein.)

Neutron PDF analysis - S. J. L. Billinge, R. G. DiFrancesco, G. H. Kwei, J. J. Neumeier, and J. D. Thompson, Phys. Rev. Lett. **77**, 715 (1996).

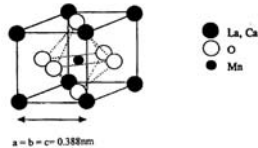
D. Louca and T. Egami, J. Appl. Phys **81**, 5484 (1997)

XAS Analysis- C. H. Booth, F. Bridges, G. H. Kwei, J. M. Lawrence, A. L. Cornelius, and J. J. Neumeier, Phys. Rev. Lett. **80**, 853 (1998).

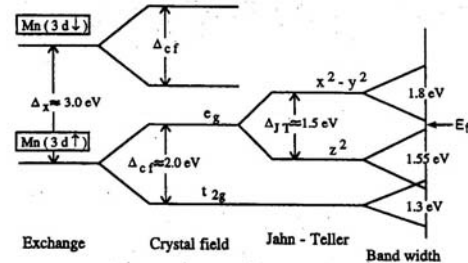
T. A. Tyson, J. Mustre de Leon, S. D. Conradson, A. R. Bishop, J. J. Neumeier, H. Röder, and Jun Zang,, Phys. Rev. B **53**, 13985 (1996).

**Changes in the Mn-O bond correlation or Mn-O bond distribution were found to track the onset of the ferromagnetic conducting state.**

## Jahn-Teller Distortions in Mn<sup>3+</sup>



Symmetric nonlinear molecule with degenerate state will distort to lower the symmetry and remove the degeneracy

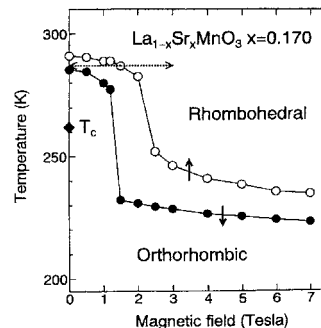


LSDA computation on LaMnO<sub>3</sub>  
S. Satpathy, Z. S. Popovic and F. R. Vukajlovic, JAP **79**, 4555 (1995)

## Spin-Lattice Coupling

It was observed that the application of an external magnetic field induced structural phase transitions in La<sub>0.83</sub>Sr<sub>0.17</sub>MnO<sub>3</sub>

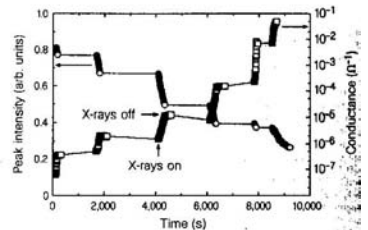
A. Asamitsu *et al.*, Nature **373**, 6513 (1995).



## Light-Charge Coupling

X-rays can destroy the insulating phase of  $\text{Pr}_{0.7}\text{Ca}_{0.3}\text{MnO}_3$  (4 K shown)

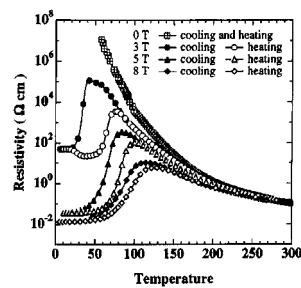
V. Kiryukhin *et al.* Nature 813, (1997).



## Spin-Charge Coupling and Lattice-Charge Coupling

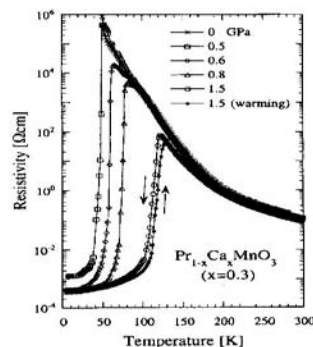
A high magnetic field can destroy the insulating phase of  $\text{Pr}_{0.7}\text{Ca}_{0.3}\text{MnO}_3$

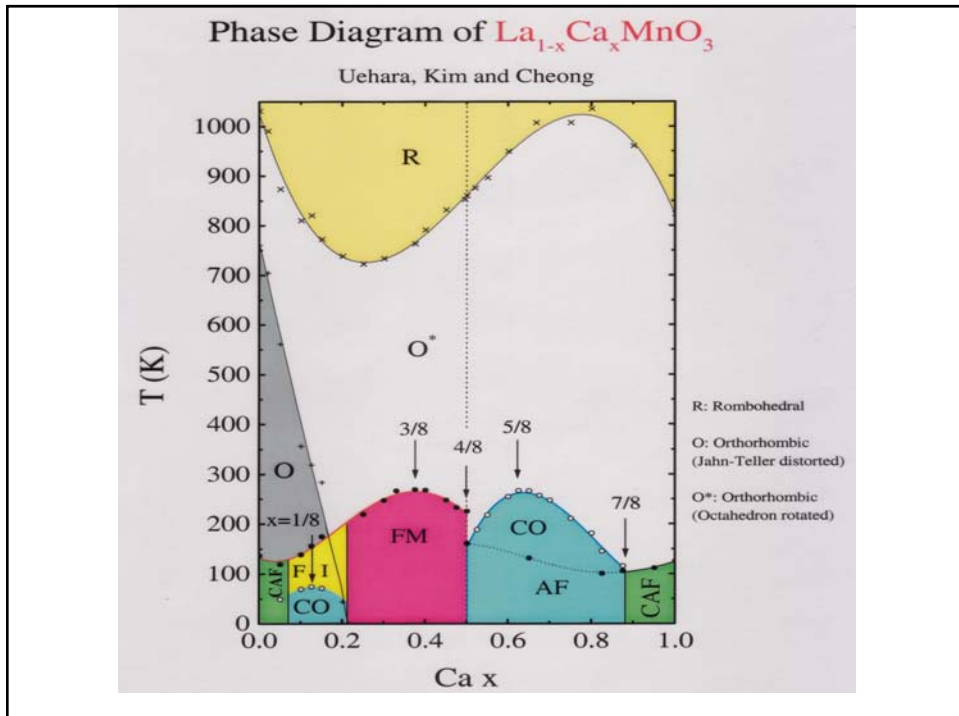
J. Barratt *et al.* APL 424, (1996).



High pressure can destroy the insulating phase of  $\text{Pr}_{0.7}\text{Ca}_{0.3}\text{MnO}_3$

Y. Moritomo, H. Kuwahara and Y. Tomioka, Phys. Rev. B 55, 7549 (1997).





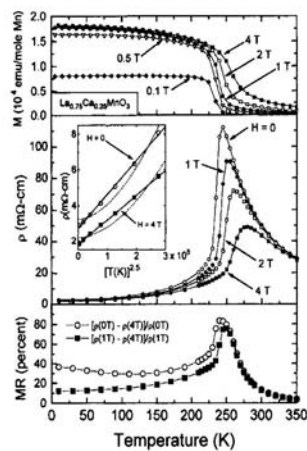
## $\text{La}_{1-x}\text{Ca}_x\text{MnO}_3$ ( $x=0.25$ ) High MR System

**Magnetization, resistivity and magnetoresistance (MR) in FM region of phase diagram with  $T_p \sim T_c$**

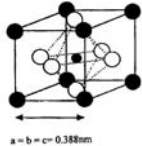
P. Schiffer, A. P. Ramirez, W. Bao and S. W. Cheong *et al.* PRLL 75, 3336 (1995)

### Problems

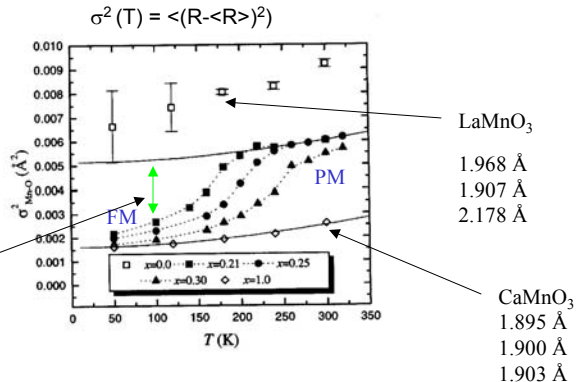
- Fields required are too high
- Temperature is too low



## Changes in Local Structure $x \sim 0.25$

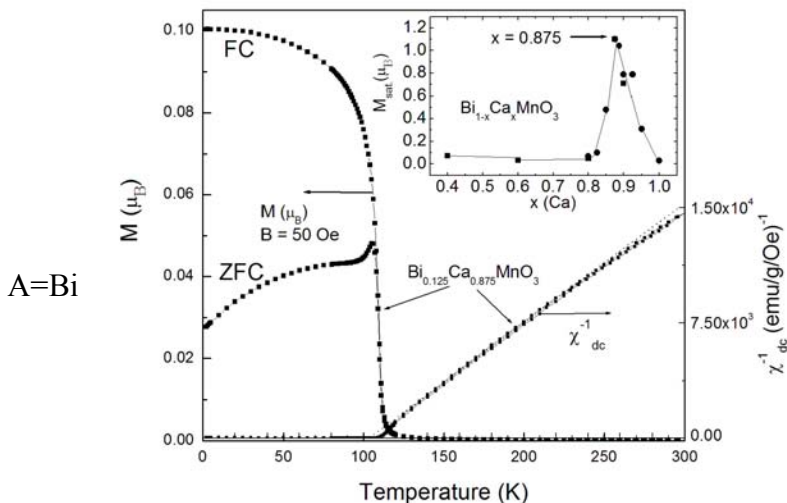


● La, Ca  
○ O  
● Mn  
  
40% change



C. H. Booth, F. Bridges, G. H. Kwei, J. M. Lawrence, A. L. Cornelius, and J. J. Neumeier, Phys. Rev. Lett. **80**, 853 (1998)

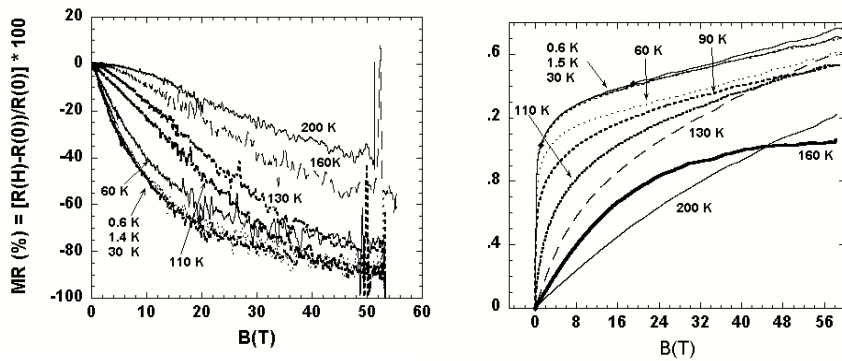
## La<sub>1-x</sub>A<sub>x</sub>MnO<sub>3</sub> ( $x=0.875$ ) High MR System



H. Woo, T. A. Tyson, *et al.* (unpublished)

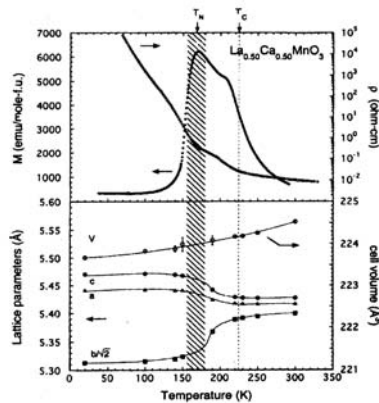
S.-W. Cheong and H. Y. Hwang, *Colossal Magnetoresistive Oxides*  
edited by Y. Tokura

## $\text{Bi}_{0.125}\text{Ca}_{0.875}\text{MnO}_3$ MR in High Field



T. A. Tyson, Y. Qin, H. Woo, M. Jaime *et al.* (unpublished)

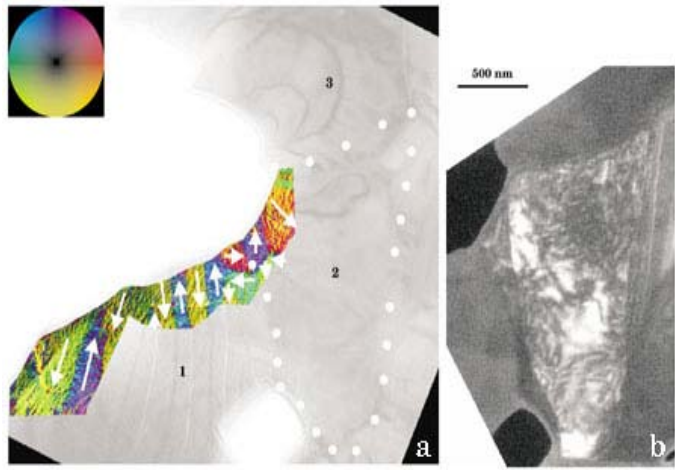
## $\text{La}_{0.5}\text{Ca}_{0.5}\text{MnO}_3$ Properties ( $x=0.5$ )



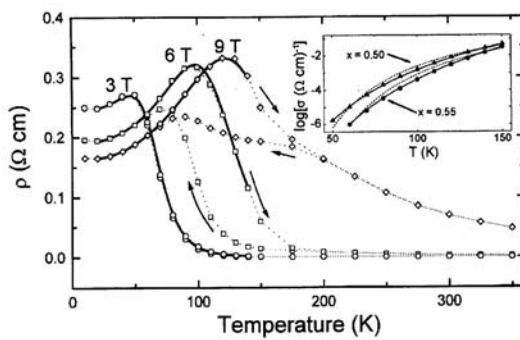
P. G. Radaelli, D. E. Cox, M. Marezio, S.-W. Cheong, P. Schiffer, and  
A. P. Ramirez, PRL 75, 4488 (1995).

## Mesoscopic Structure in $\text{La}_{0.5}\text{Ca}_{0.5}\text{MnO}_3$

Polycrystalline  $\text{La}_{0.5}\text{Ca}_{0.5}\text{MnO}_3$  exhibits macroscopic phase separation (TEM images) as can be seen in the figure on the left with 1 and 3 exhibiting ferromagnetic and charge ordered states. On the mesoscopic level, grain 2 is seen to exhibit a mixed ferromagnetic and charge ordered regions. Figures taken from N. Mathur and P. Littlewood, Physics Today, January 2003.



## $\text{La}_{0.5}\text{Ca}_{0.5}\text{MnO}_3$ Response to Magnetic Field- $\rho(T)$



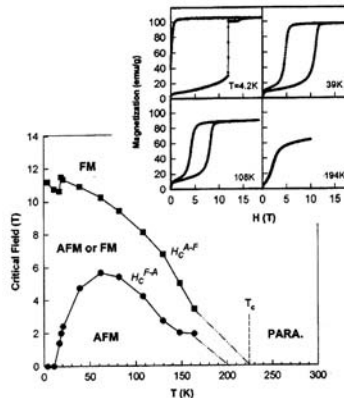
3T corresponds to  $\rho/10,000$

6T corresponds to  $\rho/25$

M. Roy, J. F. Mitchell, A. P. Ramirez and P. Schiffer, PRB **58**, 5158 (1998).

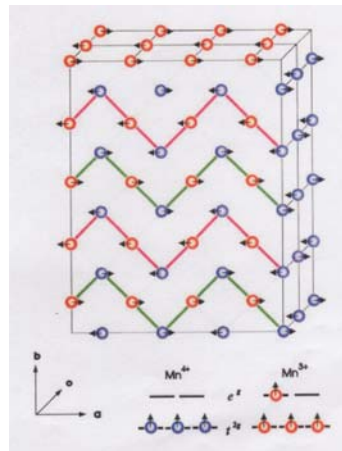
# $\text{La}_{0.5}\text{Ca}_{0.5}\text{MnO}_3$

## M(H) and Magnetic Phase Diagram



G. Xiao, E. J. McNiff, Jr., G. Q. Gong, A. Gupta, C. L. Canedy, and J. Z. Sun, PRB **54**, 6073 (1996).

## Magnetic Ordering at Low Temperature

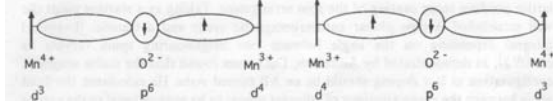


G. Xiao, E. J. McNiff, Jr., G. Q. Gong, A. Gupta, C. L. Canedy, and J. Z. Sun, PRB **54**, 6073 (1996).

## Theoretical Models - I

### Double Exchange Model (DE)

Mn site to Mn site transfer integral large  
when core  $t_{2g}$  spins are parallel  
KE of electrons minimized then Mn  
spins are parallel  
C. Zener, Phys. Rev. **81**, 440 (1951).



$$\sigma = (x e^2 / a h) (T_c / T) \\ 0.2 < x < 0.4$$

### DE generalized (general spin directions)

Mn site to Mn site transfer integral large  
when core  $t_{2g}$  spins are parallel

P. W. Anderson and H. Hasegawa, Phys.  
Rev. **100**, 675 (1955).

$$t = t_0 \cos(\theta/2)$$

- $t_0$  is bare hopping integral
- Superexchange  $\propto \cos(\theta)$   
(typically an AF interaction)

## Theoretical Models - II

### Double Exchange Model (DE)

$$H = -\sum t_0 \cos(\theta/2) c_i^\dagger c_j + J_H \sum S_i \cdot s_i$$

Explicit H for ferromagnetic  
region

$$H_{DE} = -\sum_{i,j,\sigma} t_{ij}^{ab} a_{ia\sigma}^\dagger a_{jb\sigma} + J_H \sum_{i,a_i} \vec{S}_i \cdot \vec{\sigma}_{ap} a_{ia\alpha}^\dagger a_{ia\beta} + \sum_{i,a_i} \vec{h}_{i\uparrow}^0 \cdot \vec{S}_i$$

Millis *et al.* incorporated fluctuations in  $\theta$  and were able to compute the high temperature region of the  $x \sim 0.3$  phase.

Predicted resistivity is several orders of magnitude larger than the experimental observations

Larger field required than those observed experimentally from MR systems

## Theoretical Models - III

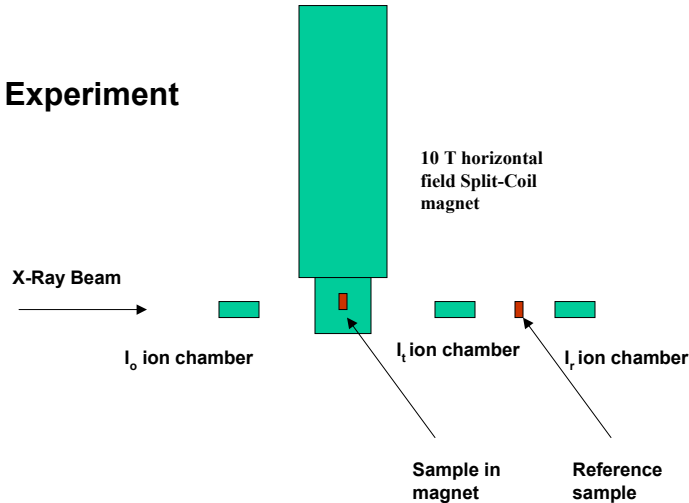
### JT Coupling to the lattice is required

- Carriers become self-trapped once strong JT included  
H. Röde *et al.*, PRL **76**, 1356 (1996).
- With this correction Millis *et al.* reproduced the resistivity observed  
A. J. Millis *et al.*, PRL **77**, 175 (1996).

$$H_{JT} = g \sum_{i,a,\sigma} a_{ia\sigma}^\dagger Q^{ab} a_{ib\sigma} + \frac{k}{2} \sum_i Q^2(i)$$

### Changes in the Local Structure of $\text{La}_{0.5}\text{Ca}_{0.5}\text{MnO}_3$ During Magnetic Field Melting of the CO State

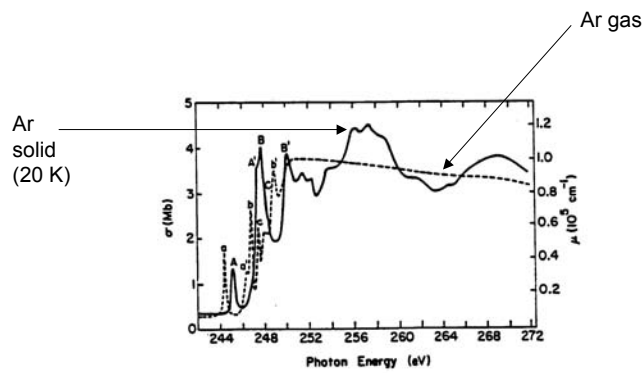
#### Experiment



## Magnet Pictures



## X-Ray Absorption Spectroscopy L<sub>2,3</sub>-Edge Edges of Gas Phase and Solid Ar (fcc)



# Relation Between Cross Section and Atomic Structure

$$\begin{aligned}
 \sigma(\hbar\omega) &= 4\pi^2 \alpha \hbar\omega \sum_{i,f} |<\psi_f|\hat{\varepsilon} \cdot \vec{r}|\psi_{core}^i>|^2 \delta(\hbar\omega + E_i - E_f) \\
 &= 4\pi^2 \alpha \hbar\omega \sum_{i,f} <\psi_{core}^i|\hat{\varepsilon} \cdot \vec{r}\delta(\hbar\omega + E_i - E_f)|\psi_f> \\
 &<\psi_f|\hat{\varepsilon} \cdot \vec{r}|\psi_{core}^i>
 \end{aligned}$$

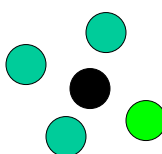
J. J. Rehr and R. C. Albers, Rev. Mod. Phys. **72**, 621 (2001) and references therein.

T. A. Tyson, K. O. Hodgson, C. R. Natoli and M. Benfatto, Phys. Rev. B **46**, 5997 (1992) and references therein.

## In Terms of the Green's Function (Scattering)

$$\begin{aligned}
 \sigma(\hbar\omega) &= 4\pi^2 \alpha \hbar\omega \sum_i \text{Im} \left[ <\psi_{core}^i|\hat{\varepsilon} \cdot \vec{r}\left[\frac{-1}{\pi} G^+(\vec{r}, \vec{r}', E)\right] \hat{\varepsilon} \cdot \vec{r}'|\psi_{core}^i> \right] \\
 &= 4\pi^2 \alpha \hbar\omega \sum_i \text{Im} \left\{ \iint d^3r d^3r' \psi_{core}^i(\vec{r}) \hat{\varepsilon} \cdot \vec{r} \right. \\
 &\quad \left. \left[ \frac{-1}{\pi} G^+(\vec{r}, \vec{r}', E) \right] \hat{\varepsilon} \cdot \vec{r}' \psi_{core}^i(\vec{r}') \right\}
 \end{aligned}$$

For a muffin-tin cluster one can  
Write down the Green's  
function



$$\frac{-1}{\pi} [G^+(\vec{r}, \vec{r}', E)]_{LL'}^{ij} = \sum_{LL'} R_L^i(\vec{r}) \tau_{LL'}^j R_L^j(\vec{r}') - \sum_L \delta_{ij} R_L^i(\vec{r}_{<}) S_L^j(\vec{r}_{>})$$

## Scattering - I

$$\sigma(\hbar\omega) = \frac{8}{3} \pi^2 \alpha \hbar\omega \operatorname{Im} \left[ {}^{(l_i+1)} \left\{ \sum_m [M_{l_i l_i}^2 \frac{1}{2l+1} \tau_{lm lm}^{00} \right. \right. \\ \left. \left. + \tilde{M}_l{}^2 \right] {}_{l=l_i+1}^{l_i+1} \left\{ \dots \right\} {}_{l=l_i-1}^{l_i-1} \right]$$

$$\tau_{lm lm}^{00} = \{ [1 - T_a G_0]^{-1} T_a \} {}_{lm lm}^{00}$$

$$\tau = [1 - T_a G]^{-1} T_a = \sum_n (T_a G)^n T_a$$

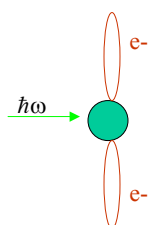
$$\tau = T_a + T_a G_0 T_a + T_a G_0 T_a G_0 T_a + T_a G_0 T_a G_0 T_a G_0 T_a + \dots$$

## Scattering - II

$$\tau = T_a + T_a G_0 T_a + T_a G_0 T_a G_0 T_a + T_a G_0 T_a G_0 T_a G_0 T_a + \dots$$

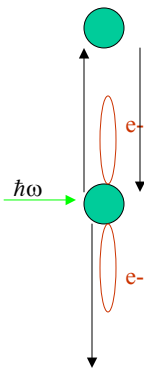
**Term 1, Atomic Absorption**

$$\sigma_l^0(\hbar\omega) \cong \sigma_{l_i+1}^0(\hbar\omega) \\ \cong \frac{8}{3} \pi^2 \alpha \hbar\omega \left( {}^{(l_i+1)} \left\{ \operatorname{Im} \left[ \sum_m M_{l_i l_i}^2 t_l^0 - \tilde{M}_l{}^2 \right] \right\} {}_{l=l_i+1}^{l_i+1} \right)$$



## Scattering III(a)

Term 3, Single Scattering



$$\begin{aligned}
 \chi_2^1(\hbar\omega) &= \frac{\sigma_1^2(\hbar\omega)}{\sigma_1^0(\hbar\omega)} \\
 &\cong \frac{\frac{8}{3}\pi^2\alpha\hbar\omega(l_{+1})}{\sigma_1^0(\hbar\omega)} \left\{ \text{Im} \left[ \sum_m M_{l_{+1} 2l+1}^2 [T_a G T_a G T_a]_{lm lm}^{00} \right] \right\}_{l=l_{+1}} \\
 &\cong \left\{ \frac{1}{\sin^2(\delta_{l_{+1}}^0)} \frac{1}{2l+1} \text{Im} \left[ \sum_m \sum_{l'm'}^l t_1^0 G_{lm l'm'}^{0r} t_1^r G_{l'm' lm}^{r0} t_1^0 \right] \right\}_{l=l_{+1}} \\
 &\cong \text{Im} \left\{ (-1)^l e^{i2\delta_{l_{+1}}^0} \sum_r \frac{e^{i2\kappa R_{0r}}}{\kappa R_{0r}^2} \sum_{l'} \frac{t_1^r, (2l'+1)p_{l'}, (\cos(\pi))}{\kappa} \right\}_{l=l_{+1}} \\
 &\cong (-1)^{l_{+1}} \sum_r \left| \sin \left\{ 2\delta_{l_{+1}}^0(\kappa) + 2\kappa R_{0r} + \arg[f(\pi, \kappa)] \right\} \right| \frac{|f(\pi, \kappa)|}{\kappa R_{0r}^2}
 \end{aligned}$$

## Scattering III(b)

$$\chi(k) = S_0^{-2} (N/kR^2) F(k, R) \exp(-2c_2 k^2 + 2/3 C_4 k^4 - 4/15 C_6 k^6) * \text{Sin}(2kR - 4/3 C_4 k^3 + 4/15 C_5 k^5 + \phi(k, R))$$

$C_n$  parameters represent distribution with small deviation away from Gaussian ( $\langle \rangle$  indicate thermal averages)

$$C_2 = \sigma^2 = \langle (R - \langle R \rangle)^2 \rangle$$

$$C_3 = \langle (R - \langle R \rangle)^3 \rangle$$

$$C_4 = \langle (R - \langle R \rangle)^4 \rangle - 3 C_2^2$$

Extracted parameters from Fit are N, R,  $C_2$ ,  $C_3$ , and  $C_4$

# Changes in Local Structure on CO Melting

- Co melting first studied by Tokura group ( $\text{Nd}_{1/2}\text{Sr}_{1/2}\text{MnO}_3$ ,  $\text{Pr}_{1/2}\text{Sr}_{1/2}\text{MnO}_3$ ,  $\text{Sm}_{1/2}\text{Ca}_{1/2}\text{MnO}_3$ ,  $\text{Pr}_{1/2}\text{Ca}_{1/2}\text{MnO}_3$  and others)
  - (a) H. Kuwahara, Y. Tomioka, A. Asamitsu, Y. Moritomo and Y. Tokura, Science **270**, 961 (1995).
  - (a) Y. Tomioka, A. Asamitsu, Y. Moritomo, H. Kuwahara and Y. Tokura, Phys. Rev. Lett. **74**, 5108 (1995).
  - (b) (c) M. Tokunaga, N. Miura, Y. Tomioka and Y. Tokura, Physica B **246-247**, 491 (1998). M. Tokunaga, N. Miura, Y. Tomioka and Y. Tokura, Phys. Rev. B **57**, 5259 (1998).
- Detailed studies have been done on the bulk properties of  $\text{La}_{1/2}\text{Ca}_{1/2}\text{MnO}_3$ 
  - (a) P. Schiffer, A. P. Ramirez, W. Bao and S.-W. Cheong, Phys. Rev. Lett. **75**, 3336 (1995).
  - (b) G. Xiao, E. J. McNiff, G. Q. Gong, A. Gupta, C. L. Canedy and J. Z. Sun, Phys. Rev. B **54**, 6073 (1996). (b) G. Xiao, G. Q. Gong, C. L. Canedy, E. J. McNiff , and A. Gupta, J.Appl. Phys. **81**, 5324 (1997).

## H-T Diagram of $\text{La}_{0.5}\text{Ca}_{0.5}\text{MnO}_3$

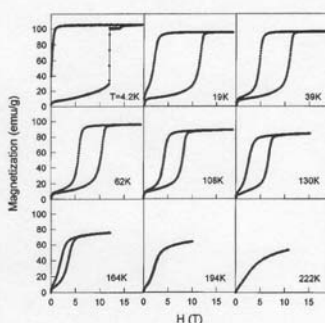


FIG. 4. Magnetization curves of  $\text{La}_{0.5}\text{Ca}_{0.5}\text{MnO}_{3+\delta}$  measured at different temperatures.

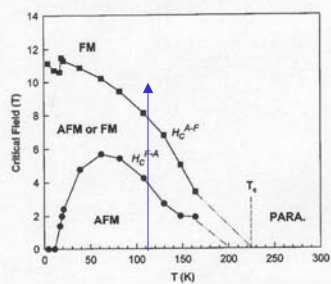
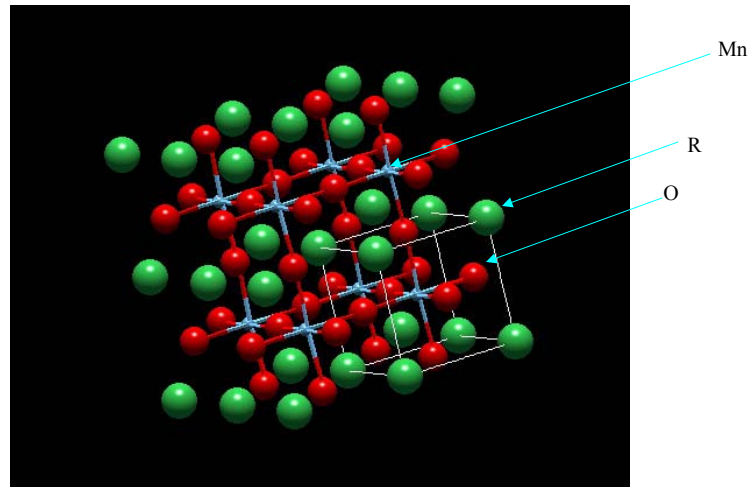


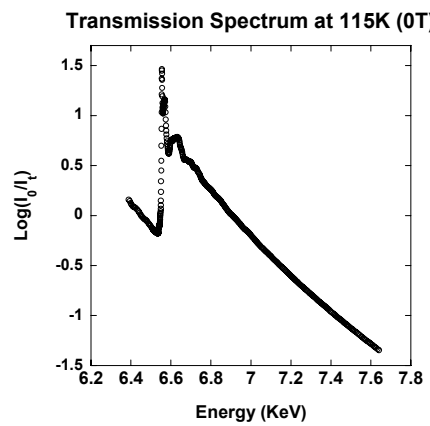
FIG. 5. Phase diagram of  $\text{La}_{0.5}\text{Ca}_{0.5}\text{MnO}_{3+\delta}$  in the  $H-T$  plane.  $H_c^{A-F}$  and  $H_c^{F-A}$  are critical fields for the AFM-FM and FM-AFM transitions, respectively. The magnetic transition temperature ( $T_c$ ) was obtained from the susceptibility measurement.

G. Xiao, G. Q. Gong, C. L. Canedy, E. J. McNiff , and A. Gupta, J.Appl. Phys. **81**, 5324 (1997).

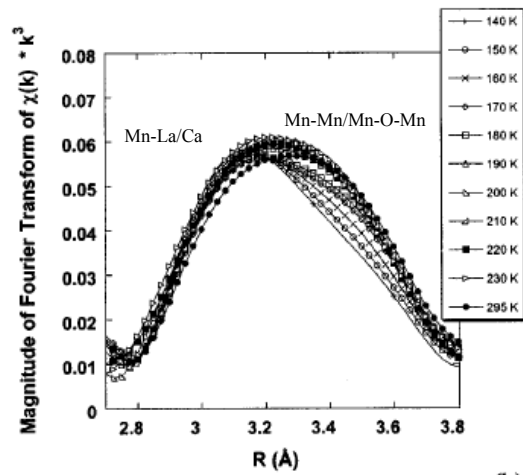
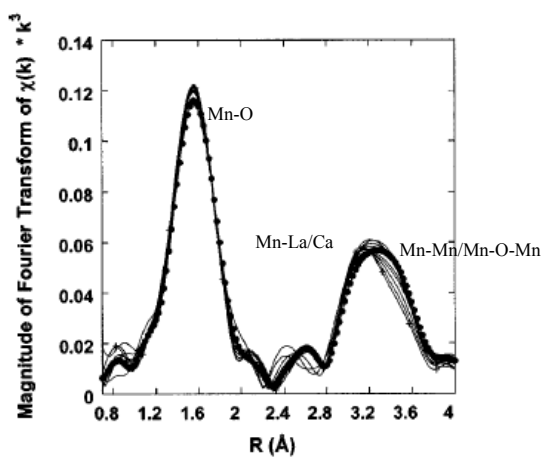
## RMnO<sub>3</sub> Crystal Structure



Raw XAFS Data (115K, H=0,  
Mn K-Edge)

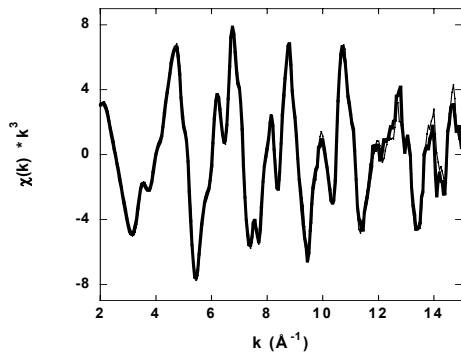


### Temperature Dependence of Structural Changes



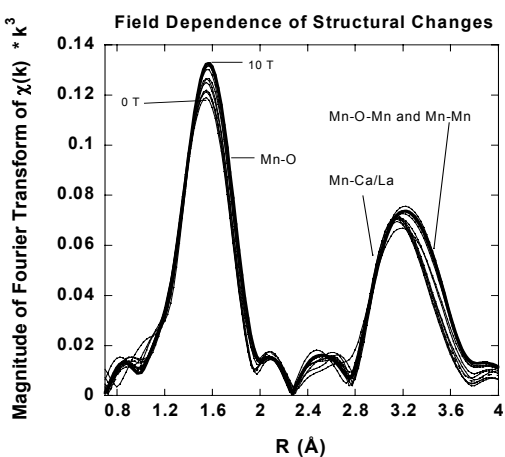
(b)

## Extracted XAFS Spectra at H=0 (T=115K)



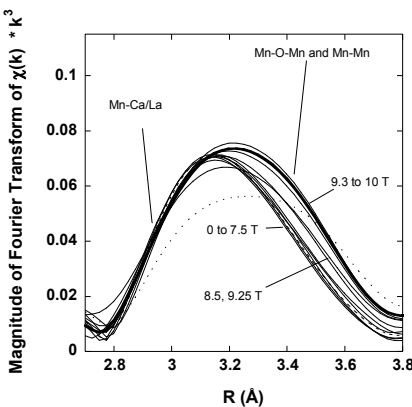
## Trends With Magnetic Field

Fourier transform of the field dependent XAFS data over the range  $2.54 < k < 14.05 \text{ \AA}^{-1}$  with the Mn-O, Mn-Ca/La and Mn-Mn/Mn-O-Mn peaks labeled.



## Trends With Magnetic Field: Mn-Mn Contribution

The expand Mn-Mn/Mn-O-Mn peak shows that three distinct structural regions exists. The 300 K spectrum is shown as the dotted line.



## Representative Fit to Extract Structural Parameters (Mn-O Bond)

$$\chi(k) = S_0^2 \left( N/k R^2 \right) F(k,R) \exp(-2C_2 k^2 + 2/3 C_4 k^4 - 4/15 C_6 k^6) * \sin(2kR - 4/3 C_4 k^3 + 4/15 C_5 k^5 + \phi(k,R))$$

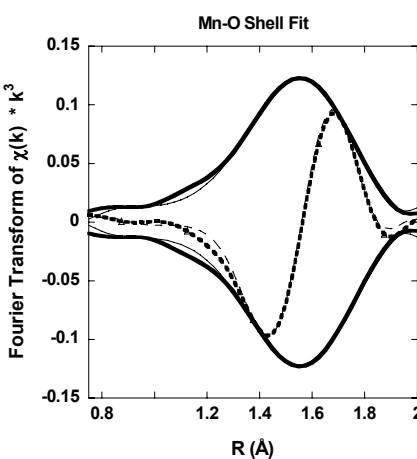
$C_n$  parameters represent distribution with small deviation away from Gaussian ( $\langle \rangle$  indicate thermal averages)

$$C_2 = \sigma^2 = \langle (R - \langle R \rangle)^2 \rangle$$

$$C_3 = \langle (R - \langle R \rangle)^3 \rangle$$

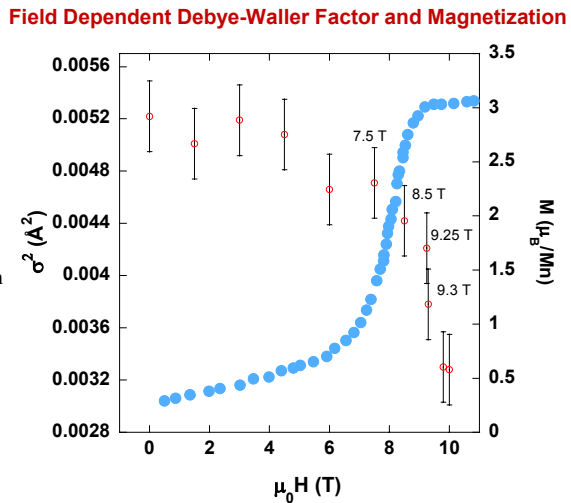
$$C_4 = \langle (R - \langle R \rangle)^4 \rangle - 3 C_2^2$$

Extracted parameters from Fit are  
 $N$ ,  $R$ ,  $C_2$ ,  $C_3$ , and  $C_4$



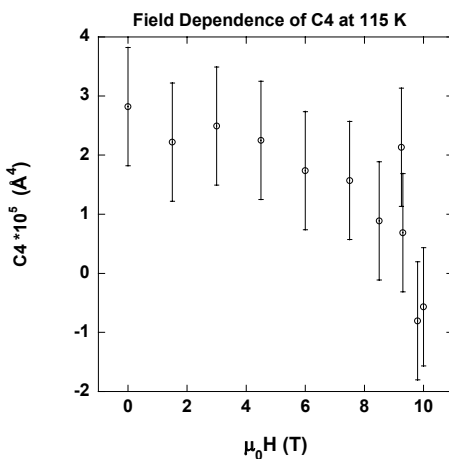
## Field Dependent Debye-Waller Factors (Mn-O Bond)

The field dependent Debye-Waller factor ( $\sigma^2 = <(R - \langle R \rangle)^2>$ , open circles) for Mn-O bond compared with the magnetization (solid dots taken from Xiao *et al.*)



## Field Dependent C4 (Mn-O Bond)

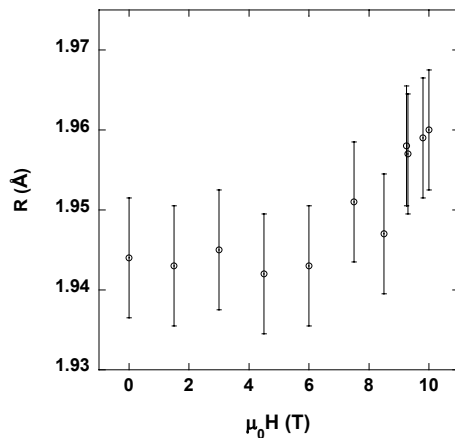
C4 vanishes resulting in a narrow Gaussian peak at high field



## Field Dependent $\langle R_{\text{Mn-O}} \rangle$

R converges to 1.96 Å value found in the metallic x=0.3 system

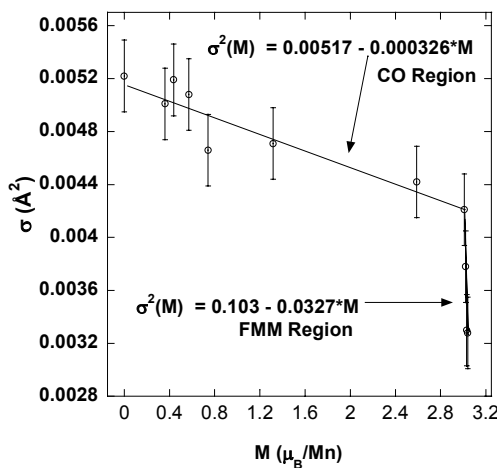
Field Dependence of Average Mn-O Distance at 115 K



## Mn-O Variance (JT) as a Function Magnetization

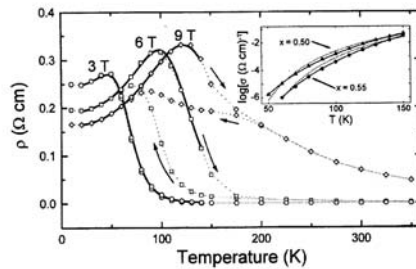
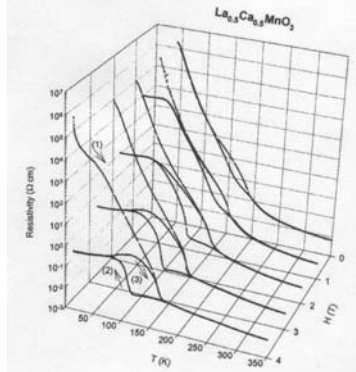
The JT distortion varies linearly in both the metallic (FMM) and charge ordered (CO) regions. The rate of change of the JT distortion is 100 times faster after crossing into the ferromagnetic metallic region.

Debye-Waller Factor vs. Magnetization



# $\text{La}_{0.5}\text{Ca}_{0.5}\text{MnO}_3$

## $\rho(T)$ in Field



3T corresponds to  $\rho/10,000$

6T corresponds to  $\rho/25$

G. Xiao, E. J. McNiff, G. Q. Gong, A. Gupta, C. L. Canedy and J. Z. Sun, Phys. Rev. B **54**, 6073 (1996).

M. Roy, J. F. Mitchell, A. P. Ramirez and P. Schiffer, PRB **58**, 5158 (1998).

# $\text{La}_{0.5}\text{Ca}_{0.5}\text{MnO}_3$

## $\rho(H)$ and $M(H)$ at Low Temperature

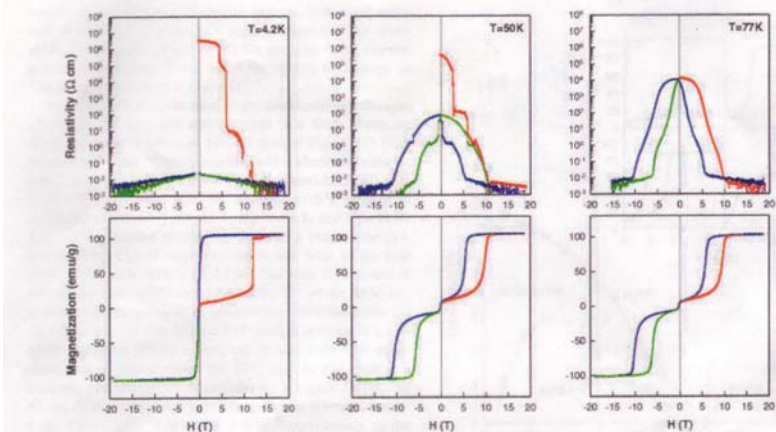


FIG. 1. Resistivity (in log scale) and magnetization of  $\text{La}_{0.5}\text{Ca}_{0.5}\text{MnO}_{3+\delta}$  versus magnetic field at  $T = 4.2, 50$ , and  $77$  K. For each run, the sample was cooled in zero field, and then subjected to a sweeping field sequence: (red)  $0 \rightarrow 19$  T; (blue)  $19$  T  $\rightarrow 0 \rightarrow -19$  T; (green)  $-19 \rightarrow 0 \rightarrow 19$  T.

G. Xiao, E. J. McNiff, G. Q. Gong, A. Gupta, C. L. Canedy and J. Z. Sun, Phys. Rev. B **54**, 6073 (1996).

## Summary

- At high field the local JT collapses un-trapping  $e_g$  electrons and an abrupt drop in resistivity at low temperature occurs (smoothed out at high T)
- The linear regimes of variance in Mn-O vs M exist
- Jumps in resistivity with field are possibly attributed to progressive local structural changes (Mn-O JT, Mn-O-Mn buckling).
- We suspect that these jumps may be a common feature of CO systems which should be explored

## Acknowledgments

Data acquisition was performed at Brookhaven National Laboratory's National Synchrotron Light Source (NSLS) which is funded by the U. S. Department of Energy. The magnet acquisition funded by NSF IMR Grant DMR-0083189 and operational costs were funded by NSF DMR-0209243. Sample preparation was supported by NSF DMR-9802513 (SWC).